International Journal of Environmental Research (2020) 14:393–402
https://doi.org/10.1007/s41742-020-00265-2

RESEARCH PAPER

Efficiency Enhancement of Dye-Sensitized Solar Cells Based on Gracilaria/Ulva Using Graphene Quantum Dot

Afsoon Saedi[1] · Ali Mashinchian Moradi[1] · Salimeh Kimiagar[2] · Homayon Ahmad Panahi[3]

Received: 28 December 2019 / Revised: 22 April 2020 / Accepted: 30 April 2020 / Published online: 4 June 2020

Abstract

Dye-sensitized solar cells (DSSC) have been assembled using natural dyes extracted from the red (Gracilaria) and green (Ulva) algae as photosensitizers and the effect of adding Graphene quantum dot (GQD) has been investigated. The open-circuit voltage (V_{OC}) values of natural dyes of Gracilaria, Gracilaria + GQD, Ulva, and Ulva + GQD are 0.64, 0.73, 0.70, and 0.75, respectively. The short circuit current density (J_{SC}) values are varied from 0.96 to 2.26 mA cm^{-2}, and the fill factor (FF) from 52 to 56% for the mentioned samples. The best-energy conversion efficiency of approximately 0.94% has been achieved for DSSC with Gracilaria + GQD with J_{SC} equal 2.26 mA cm^{-2}, V_{OC} is 0.73 V, and FF is 56%.

Article Highlights

- **Dye-sensitized solar cells were assembled using red (Gracilaria) and green (Ulva) algae.**
- **The results showed that adding the Graphene quantum dot to dye as a sensitizer increased significantly the efficiency.**
- **The best energy conversion efficiency of approximately 0.94% was achieved.**
- **To the best of our knowledge, there is no report for this kind of solar cell.**

Keywords Dye-sensitized · Solar cells · Gracilaria · Ulva · Graphene quantum dot

Introduction

One of the most critical challenges in the recent years is the supply and finding new sources of energy (Sathiyan 2016; Najafi and Kimiagar 2018; Wang 2004). Hence, the use of available and affordable energy sources, such as solar energy has expanded rapidly. A dye-sensitized solar cell (DSSC) is a kind of photo-electrochemical solar cell, which has attracted extensive attention due to wide-ranging operative advantages, such as low-priced materials, accessible manufacturing technology, printable, and flexible usage (O'Regan and Grätzel 1991; Bach 1998; Kuang 2008). Today, many researchers developing this type of solar cells has focused on synthesizing large bandgap semiconductor as the electrodes, finding new stable absorbing visible light dyes (Bessho 2010; Hu and Robertson 2016), and effective electrolytes (Hao 2016). Meanwhile, the Ruthenium and Osmium complexes are used more efficiently in metal–organic dyes, but these complexes are so expensive and need multistep reactions (Nazeeruddin 2001; Argazzi 2004). Therefore, finding a simple and affordable methods for preparation of sensitizer dyes is among the most important research topics in this field. The natural dyes and their organic derivatives provide a viable candidate due to their unique features, such as nontoxic synthesis, earth-abundant, low-cost elements, renewable, and environmentally friendly (Calogero 2012, 2010; Calogero and Marco 2008). There are numerous reports in the literature that applied various natural dyes as sensitizers in DSSC, which extracted from algae, flowers, fruit, and

✉ Ali Mashinchian Moradi
mashinchian@gmail.com

[1] Faculty of Natural Resources and Environment, Science and Research Branch, Lslamic Azad University (IAU), Tehran, Iran

[2] Nano Research Lab (NRL), Physics Department, Central Tehran Branch, Islamic Azad University, (IAU), Tehran, Iran

[3] Chemistry Department, Central Tehran Branch, Islamic Azad University, (IAU), Tehran, Iran

leaves (Narayan 2012; Hao 2006; Smestad 1998; Dai and Rabani 2002). For example, Calogero et al. (2015) have reported photovoltaic performance in DSSC with Chlorophyll, Anthocyanin, and Betalain as a natural sensitizer dye. However, unfortunately, the natural dye-sensitized solar cells do not have significantly open-circuit current due to the recombination of the dye molecules–TiO_2 at the interface. During the recombination process, after dye excitation by photons and before the electrons transferred from dye molecule to the TiO_2, the relaxation of the excited states occurs. Therefore, more separation of electron–hole after excitation has an essential role in increasing the current. It is well known that the Graphene quantum dot (GQD) is one of the great candidates for reducing recombination and increasing electron–hole separation (Paulo et al. 2016; Ali 2015; Ho et al. 2016). The quantum confinement effect in GQD nanoparticles generates exceptional electronic and optical properties due to their size. Comparing the bulk, orbitals alignment, and electronic structure in the nano-sized GQD varied expressively. Thus, light absorption and excited state transportation exist much longer leading to strong fluorescence upon illumination. These characteristics result in full applications of GQD in different fields, such as photovoltaics (Kongkanand et al. 2008; Zhao et al. 2007). Effective photocarrier generation with a high separation rate at the metal–oxide interface appears due to low dimension of GQD, which also reduce the recombination rate of charges (Long 2013). Besides, researches have shown that GQD enhances the optical spectrum of dye absorption, and has been widely used in DSSCs (Gupta et al. 2011). Fang et al. reported the role of adding GQDs on optical properties in a typical DSSC (Fang et al. 2014). They indicated that the amount of dye adsorption increased due to increasing of the GQD. The role of GQDs as co-sensitizers in DSSC designs with the purpose of light-harvesting enhancement, focusing on various compatible mechanisms (i.e., charge transfer, energy transfer, and recombination rate) has been explored by Mihalache et al. (2015). Kundu et al. reported enhancing the efficiency of DSSCs using N, F, and S, co-doped GQDs. They reported enhanced power conversion efficiency (Kundu et al. 2017).

The marine seaweeds have gained attention, due to dyes present in the seaweeds and could be alternative sensitizers. The most commonly used sensitizers are metal complexes that are less available and more expensive. Metal-free organic dyes with trust efficiency can be considered as potential alternatives for metal complexes due to their high-molar extinction coefficient, simple synthesis, and lower cost.

In this study, DSSC was assembled using natural dyes extracted from red and green algae as a sensitizer and the effect of adding GQD to natural dyes on DSSC performance has been investigated. Furthermore, photocurrent–voltage characteristics in the presence and absence of GQD have been studied.

Experimental Section

Pigment Extraction

The Gracilaria (red algae) and Ulva (green algae) have been collected from intertidal and subtidal areas in Chahbahar (Iran) and Kish Island (Iran), respectively. A portion of each sample was dried in the sun and then smashed to obtain a soft powder. 20 ml ethanol was added to the sample, and the solution was stirred, and then filtered. In the next step, 20 ml petroleum ether was added to the solution, and transferred to a separatory funnel to remove ethanol.

Cell Fabrication

All chemical materials used for the experiments were purchased from Merck Company. The GQDs (lateral dimensions < 100 nm) in the form of 1 mg/mL suspension in H_2O were purchased from Merck. To make anode, first coated fluorine-doped tin oxide on the glass substrate (FTO, 15 Ω/sq.) was cleaned with soap, ethanol, and deionized water. Then, a thin film of TiO_2 as a window layer spin-coated on the substrate by using 0.4 M $TiCl_4$ in ethanol then annealed at 180 °C for 30 min. In order to provide the TiO_2 paste, 3 g TiO_2 (anatase phase) and 3 g polyethylene glycol (PEG) were added to 100 mL ethanol, and mixed in a shaker at 40 °C for 3 h according to Najafi et al. (2017). In the next step, the porous TiO_2 layer on the substrate obtained using TiO_2 paste by the doctor blade coating method, and annealed at 600 °C for 30 min. The anodes were floated in natural dye solutions and natural dye solutions with GQD for 24 h, and then the anodes were dried at room temperature. A few nanometers thick platinum (Pt) layers were deposited on to the FTO as a counter electrode (cathode). Finally, the electrolyte was I^-/I_3^- injected to transfer the electrons between TiO_2 and the counter electrode.

Mechanism

A schematic picture of a typical DSSC mechanism is shown in Fig. 1. In Eq. (1) dye molecule (D), upon photon absorption, is promoted to an electronically excited state (D*).

$$D + h\upsilon \Rightarrow D^* \quad (1)$$

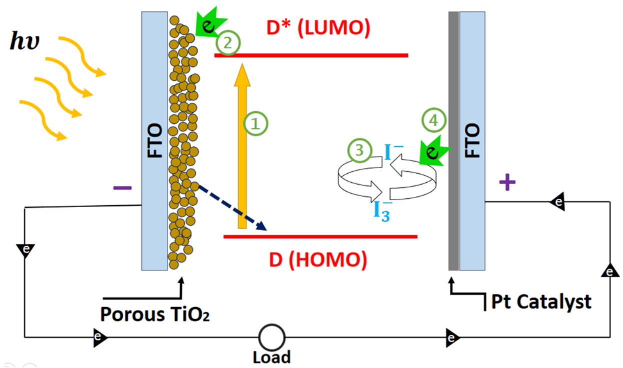

Fig. 1 Schematic of electron transfer processes in DSSC

In Eq. (2), the excited dye molecule injects an electron into the TiO_2 conduction band due to the higher conduction band (CB) edge.

$$D^{*} + TiO_2 \Rightarrow D^{+} + e^{-}\left(\mathrm{to}TiO_2\right) \quad (2)$$

The oxidized dye molecule (D^{+}) is then regenerated by a redox electrolyte, such as I^{-}/I_3^{-} couple according to Eq. (3).

$$2D^{+} + 3I^{-} \Rightarrow 2D + I_3^{-} \quad (3)$$

The injected electrons in the external circuit generate a current flow, which provides a reduction in iodine species at the counter electrode, according to Eq. (4).

$$I_3^{-} + 2e^{-}(\text{from Pt}) \Rightarrow 3I^{-} \quad (4)$$

Thus, in this circumstance, the entire cycle is regenerative and the overall balance of the process will be the conversion of photons to electrons without any permanent chemical transformation.

Results and Discussions

Anode Characterization

The X-ray diffraction pattern of porous TiO_2 paste on the FTO glass is shown in Fig. 2. Anatase TiO_2 single phase was detected according to (101), (103), (101), (004), (200), and (105) planes (JCPDS NO. 21-1272). The sharp intensity of the peaks shows that the porous anatase TiO_2 nanoparticles have high-quality crystalline growth. Some peaks of the rutile phase are also observed in the XRD pattern, which appeared due to the phase transition of heated TiO_2 nanoparticles in the annealing process. The average crystallite size determined from Scherer's formula (Patterson 1939) was in the range of 10–20 nm.

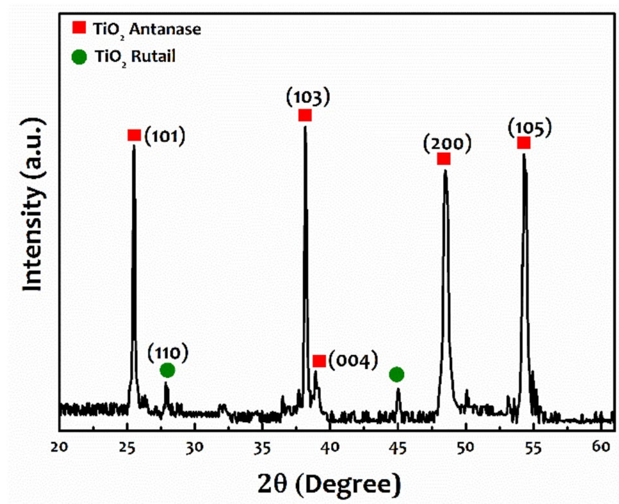

Fig. 2 XRD pattern of porous anatase TiO_2 paste on the FTO substrate

Furthermore, Fig. 3 shows the morphology of the porous TiO_2 paste on the FTO substrate which analyzed by a high-resolution scanning electron microscope (SEM). As it is seen, there are many fine pores produced in the coatings because PEG contained in the deposited layer is decomposed completely at 600 °C. The size of the pores is about 200–400 nm, which related to the amount of the added PEG. This porosity in the anode increases the interface between the dye molecules and TiO_2 and increases the electron transfer in Eq. (2).

Dye Properties

The absorption spectra of the natural dyes extracted from the red and green algae in ethanol solution are shown in Figs. 4 and 5. A competent sensitizer element should have the light-absorbing properties over a broad range, preferably from the visible to the near-infrared spectrum with the electronic excitation energy state above the CB edge of the TiO_2. From figures, it is seen that there is an absorbent peak at about 530 nm for extracts of Gracilaria and chlorophyll-containing dye extracted from Ulva have an absorption maximum at 420 nm. Since Gracilaria has a broad absorbent peak from red to blue in the visible region, it is projected to be a highly efficient sensitizer for large bandgap semiconductors. It is clear that the absorption of natural dyes + GQD in the visible range has significantly increased for both samples. A shift in the absorption edge of the dyes + GQD has appeared that causing an increase in the absorption region for this sensitizer. The red shift would be due to the structural and electronic properties of the materials, such as the photo-darkening effect. In addition, the transfer of charges takes place by GQD influences the absorption edge.

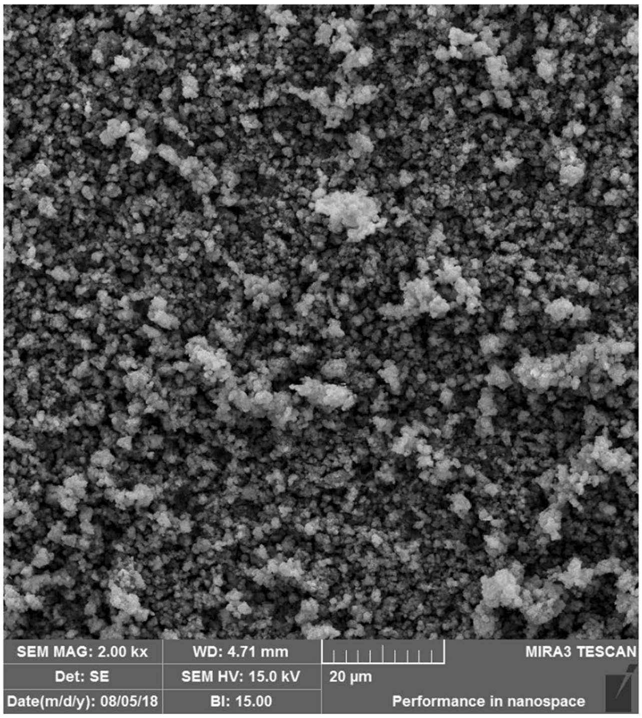

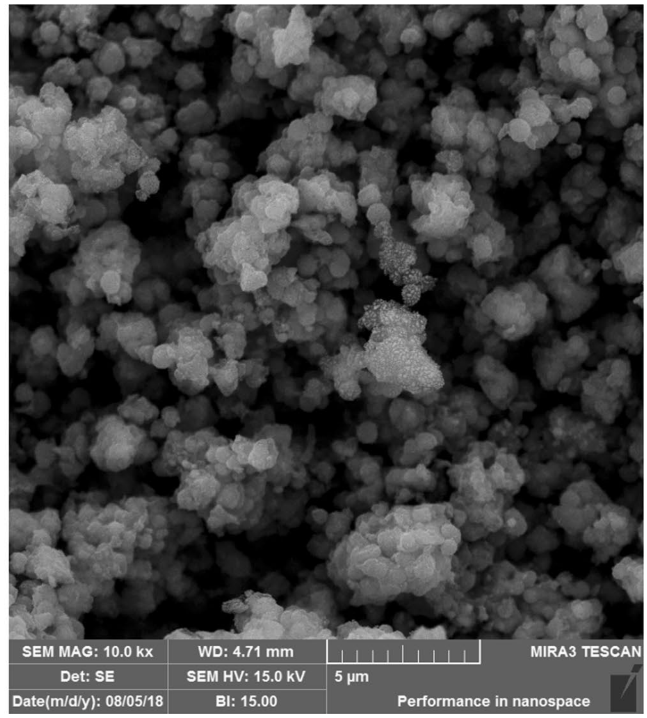

Fig. 3 SEM images of the porous TiO_2 paste on the FTO substrate

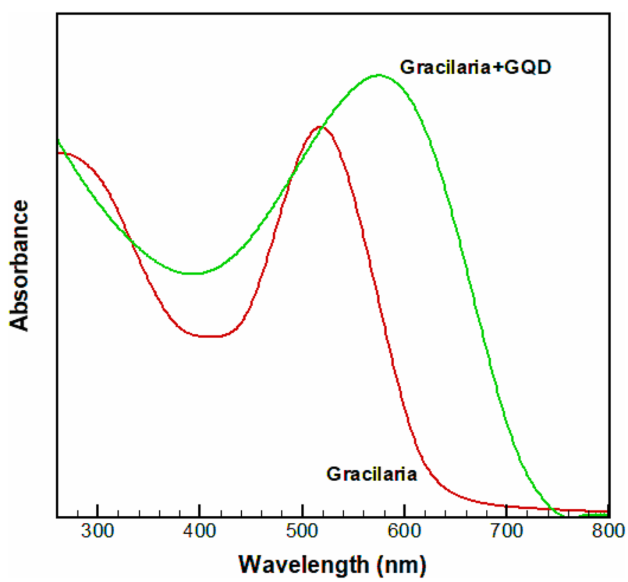

Fig. 4 Absorption spectra of the Gracilaria and Gracilaria + GQD in ethanol solution

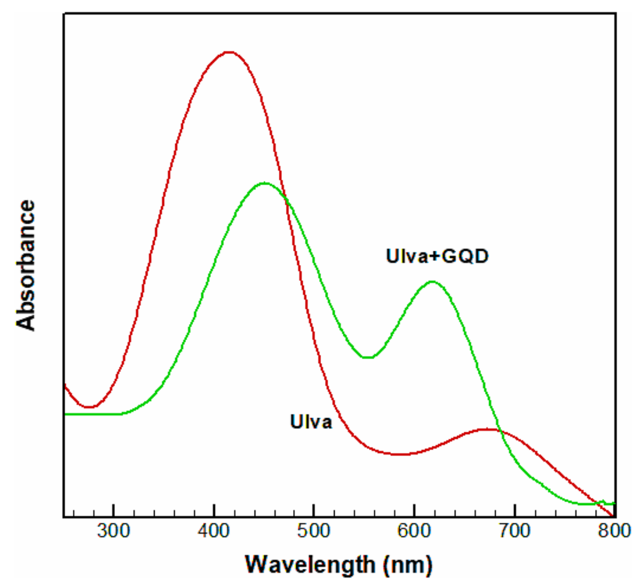

Fig. 5 Absorption spectra of the Ulva and Ulva + GQD in ethanol solution

The high absorbance, which is evident in the UV region is associated with the π–π* transition of aromatic sp^2 domains in GQD (Peng et al. 2012). The visible light absorption is due to the excitation between σ and π orbital to the lowest unoccupied molecular orbital (Riesen et al. 2014).

There are many reports that indicated adding graphene-based material into a light absorbent is expanded the light absorption to longer wavelengths. For example, Nguyen-Phan et al. showed that adding graphene oxide into TiO_2 leads to light absorption extended (Nguyen-Phan et al. 2011). Their results verify the significant influence of graphene oxide on the optical properties of TiO_2, showing band gap narrowing by increasing graphene oxide content. However, the UV–Vis absorption spectrum of GQD is included a typical π–π* transition absorption peak due to the aromatic sp^2 domains, n–π* transition absorption peak, and a long tail extending into the visible range (Zhu et al. 2015). In particular, when the GQD was added to the dyes, they modified the HOMO–LUMO gap so that it causes faster electron extraction with the presence of GQD than without its presence (Zhu et al. 2014). This means that the small amount of GQD had an influence on the total absorbance.

It is evident that after introducing GQD in the dye, Ulva + GQD absorption intensity is enhanced, and Gracilaria + GQD absorption is extended to 800 nm, which is excellent for the absorption of sunlight visible wavelength.

The bandgap of GQD is strongly influenced by its size owing to the quantum confinement effect (Ritter and Lyding 2009; Lu et al. 2011). The bandgap of the GQD increases as the size of the GQD decreases. The bandgap is determined by using the equation (Aghelifar and Kimiagar 2018):

$$\alpha = \frac{A\left(h\upsilon - E_g\right)^n}{h\upsilon} \tag{5}$$

where $h\upsilon$ is the photon energy, E_g is the optical bandgap, α is the absorption coefficient, and A is the constant, which is related to the effective masses associated with the valence and conduction bands. The $n = 1/2$ and $n = 2$ are allowed for direct and indirect transitions, respectively.

Several physical factors affect the GQD bandgap and make its type direct or indirect. The initial level ordering in the bulk material from which the dot is synthesized, the method of GQD fabrication, the size of the quantum dot, strain changes, growth technique, and quantum confinement affect the type and amount of the GQD bandgap. Different values of GQD bandgap have been reported in several studies. Senlin Diao et al. have reported optical bandgaps to

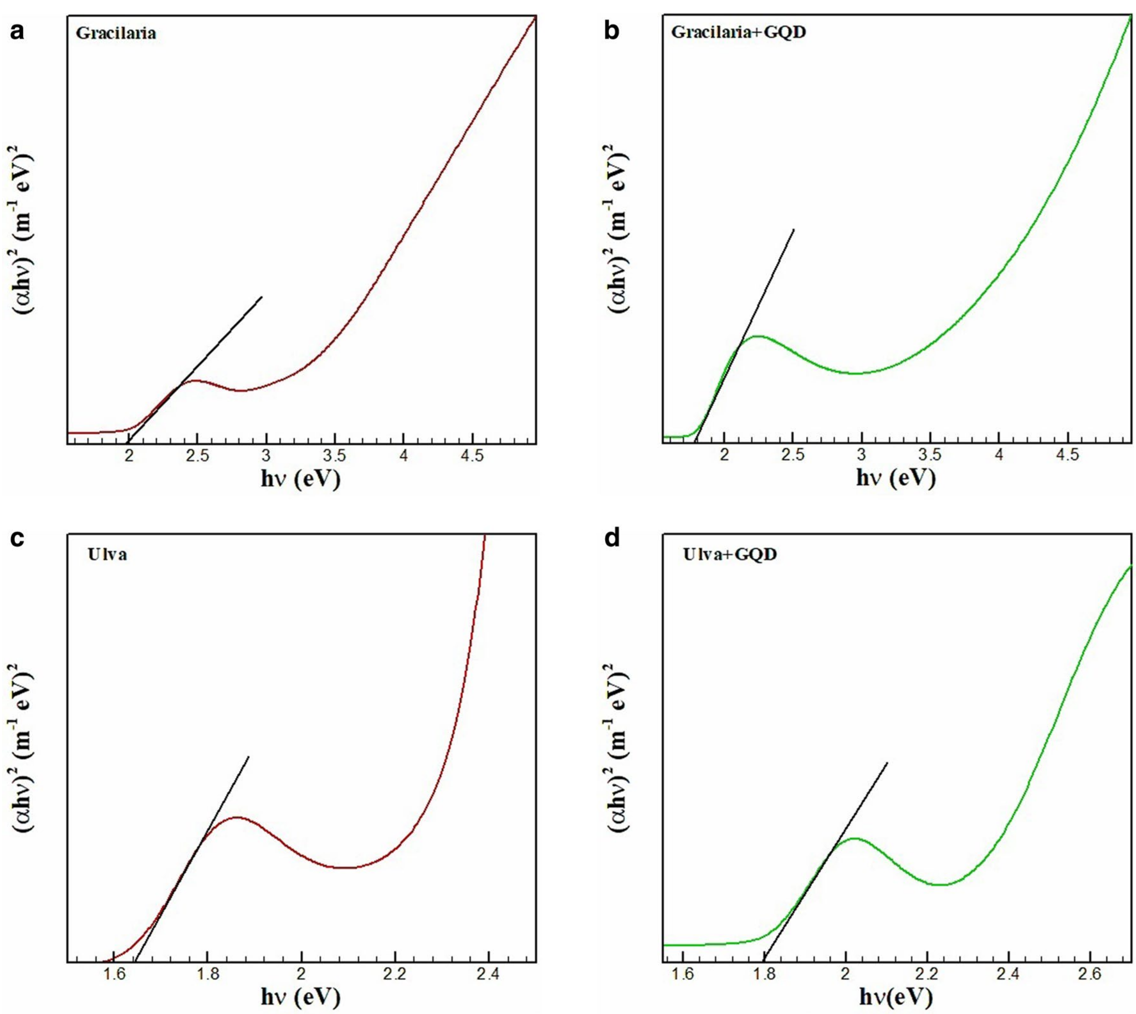

Fig. 6 Direct bandgaps of the samples

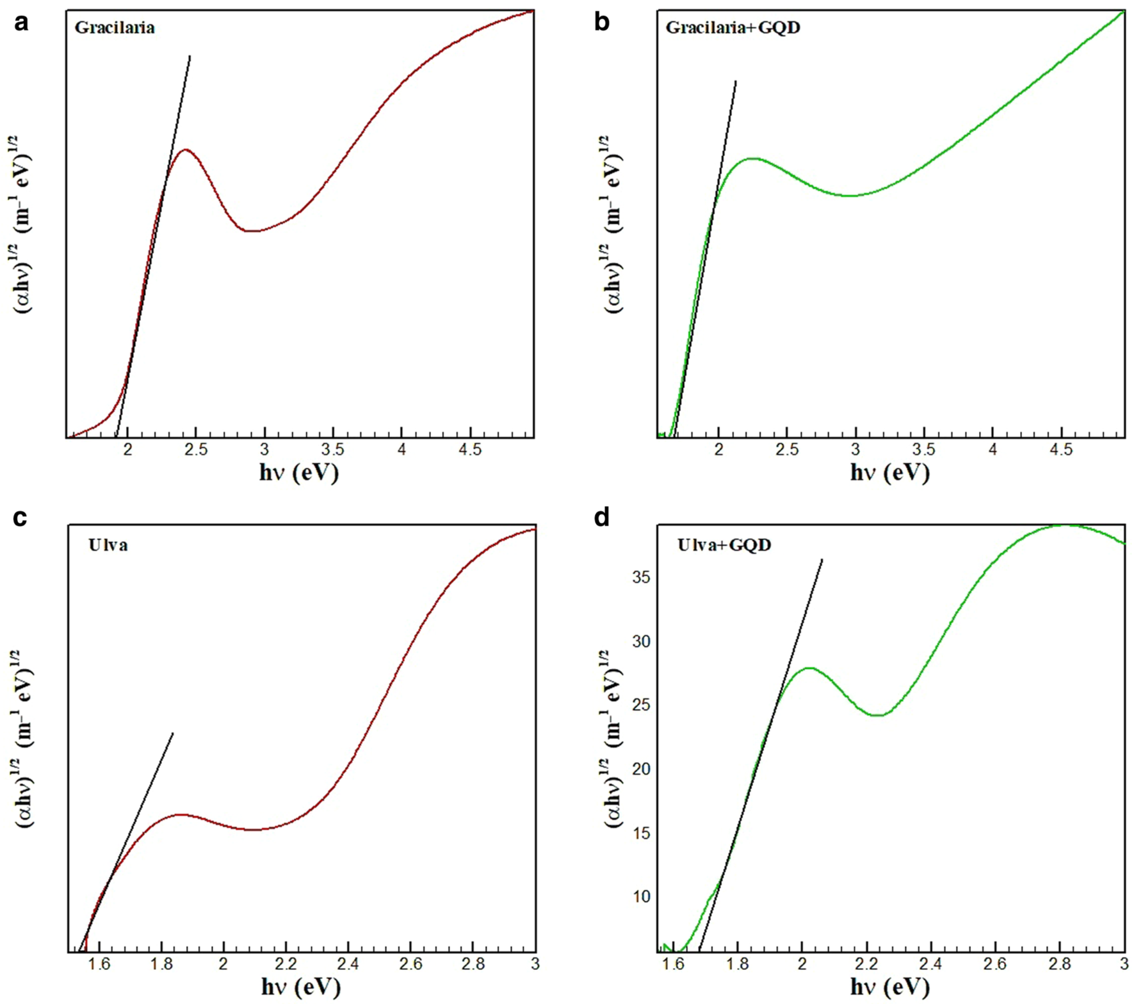

Fig. 7 Indirect bandgaps of the samples

Table 1 Bandgap estimation from Figs. 6 and 7

Sample	Gracilaria	Ulva	Gracilaria + GQD	Ulva + GQD
Direct bandgap (ev)	2	1.65	1.8	1.8
Indirect bandgap (ev)	1.9	1.55	1.5	1.7

be ~ 3.60 eV, ~ 2.93 eV, and ~ 2.27 eV for various sizes (Diao et al. 2017). To study the type of bandgap, both direct and indirect bandgaps are considered, and the results are shown in Figs. 6 and 7. It is obvious that the calculated direct bandgap is compatible with the UV results (Figs. 4 and 5). The bandgap estimation is shown in Table 1.

The transmission electron microscopy (TEM) images of natural dyes and dyes + GQD are shown in Fig. 8. As it is seen in the figures, the GQDs have been broadcast in dye uniformly. In addition, it is obvious the GQDs have a uniform size distribution with lateral dimensions smaller than 10 nm.

The photoluminescence spectrum of GQD under excitation by 334 nm wavelength is shown in Fig. 9. As reported, the fluorescence effect arises from the defect state emission (surface energy traps) and intrinsic state emission (electron–hole recombination, quantum size effect) (Zhu et al. 2011). Zhum et al. have explained that the blue emission is related to electron–hole recombination or quantum size effect (Zhu et al. 2012). The localized electron–hole pairs in the initial epoxy and carboxylic functions regularly induce nonradiative recombination and restrain pristine emission. The intrinsic state emission due to surface modification plays a significant role in PL behaviors. On the other hand, carbonyl and epoxy were transformed into –OH groups in GQD, helping suppress nonradiative processes, and further improve the integrity of the π-conjugated system as an electron donator. Typically, the fluorescence properties can be

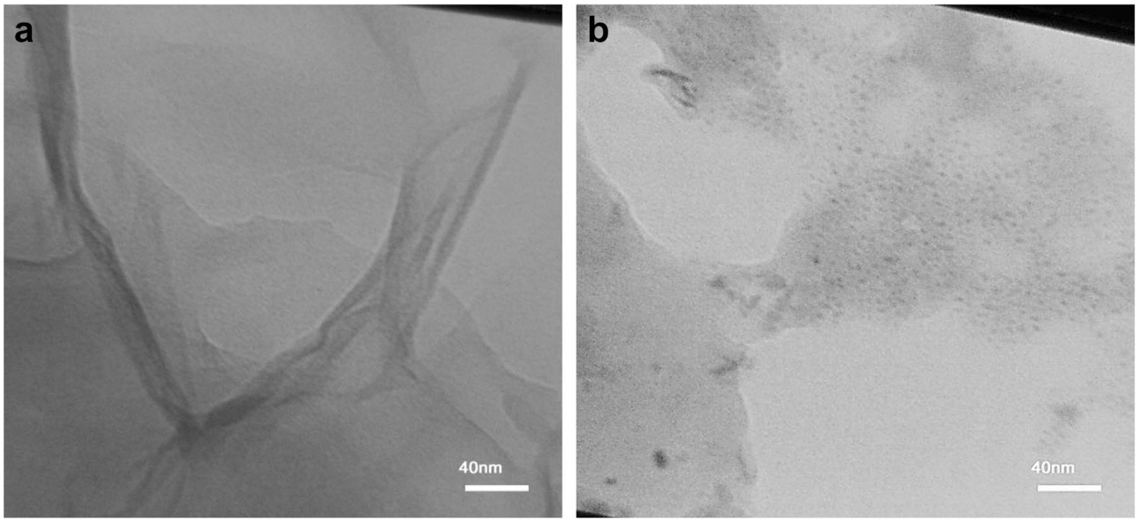

Fig. 8 TEM images of **a** the natural dyes and **b** dyes + GQD as photosensitizers

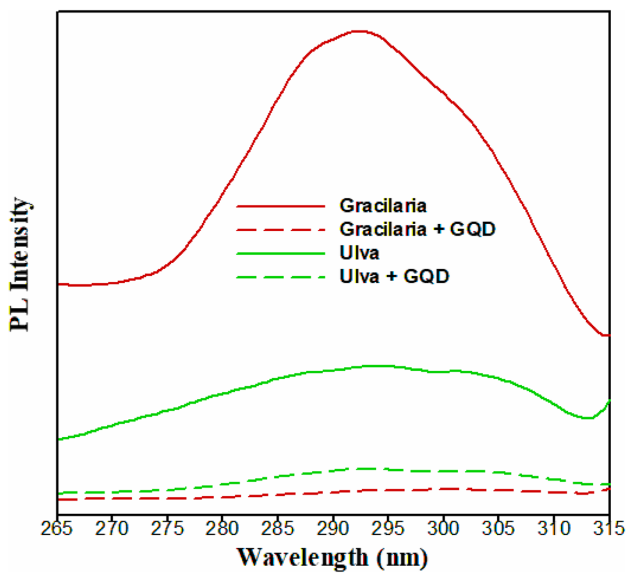

Fig. 9 Photoluminescence spectrum of dyes and dyes + GQD

adjusted and reduced by modification of GQD chemistry at the surface.

As it is seen from Fig. 9 after introducing GQD to dyes, the intensity of the PL peaks decreases remarkably, meaning the reduction in electron–hole recombination. This reduction in Gracilaria + GQD is more than Ulva + GQD. Therefore, higher efficiency is expected for solar cells based on Gracilaria + GQD.

The direct contact with the hole transporting material typically avoided by the deposition of the blocking layer on top of the FTO. The most commonly used semiconductor metal oxide is mesoporous anatase TiO_2 with a particle size of around 20–30 nm. To absorb a large amount of sensitizer, a high-surface area TiO_2 nanostructures are required. The light-absorbing sensitizer is one of the most critical fragments of any DSSC. As known in DSSC, the holes' mobility is regularly higher than the mobility of electrons in mesoporous TiO_2. However, another operative parameter is the thickness of the overlying layer and can cause high resistance in the solar cell if the thickness is not adjusted correctly. The thin layer also makes thin pinholes in contact with the metal and the mesoporous TiO_2 film (Wallace 2009; Snaith and Grätzel 2007). The conduction band contains the generated electrons through bandgap excitation, and the generated holes are located in the oxidized dye. Fast electron transportation and diffusion to the FTO electrode depend on the semiconductor electronic structure (Kroeze et al. 2006). The oxidized dye can be regenerated in the electrolyte and achieves the charge transport to the electrode via diffusion (Wu et al. 2015). The sufficient protection on the TiO_2 electrode also provided by dye molecules, which reduce interfacial recombination and permit for an upward shift in the TiO_2 conduction band by their substantial dipole moment. Consistently, dye molecules facilitate the wetting process of the hole transporting material within the mesoporous structure. The dipole moment of organic dyes can also be affected by small molecules adsorbed on the TiO_2 surface parallel to the conduction band edge (Schmidt-Mende et al. 2005). The carboxyl in GQD as an acceptor group is for binding (π-bridge) to the metal oxide semiconductor. In the dye molecule, the donor part comprises the electron density of the highest occupied molecular orbital (HOMO), whereas the acceptor fragment is the density of the lowest unoccupied molecular orbital (LUMO) (Mahmood 2016). During the photoexcitation process of the dye, the electrons can be transferred from the donor part to the acceptor through the π-bridge. Thus, charge injection and dye regeneration can be ensuing by this conformation, which lets the electrons and holes be separated in the dye molecule after light excitation.

Photovoltaic Performance of Cell

In order to investigate the photovoltaic properties of red and green algae-based dye-sensitized solar cells, the current density–voltage (*J–V*) curve under 1 kW/m^2 simulating AM1.5 irradiation plotted which is shown in Fig. 10. Open-circuit voltage V_{OC} shows the output voltage of the solar cell when there is no current density. The V_{OC} is the potential difference between the Fermi levels of electrons and holes in the film and the transporting material, respectively.

Similarly, the photocurrent density (J_{SC}) is determined based on the incident light to produce efficiency concerning the surface area and the charge injection and collection efficiencies. The short circuit current I_{SC} is recorded at zero potential and commonly normalized by the solar cell area to give a more comparable short circuit current density J_{SC}. FF is a measure of the solar cell quality, which is the ratio of the actual maximum available power to the product of the open-circuit voltage and short circuit current. This is a key parameter in evaluating performance, which is obtained from the following equation (Wolf 1971; Gray 2020):

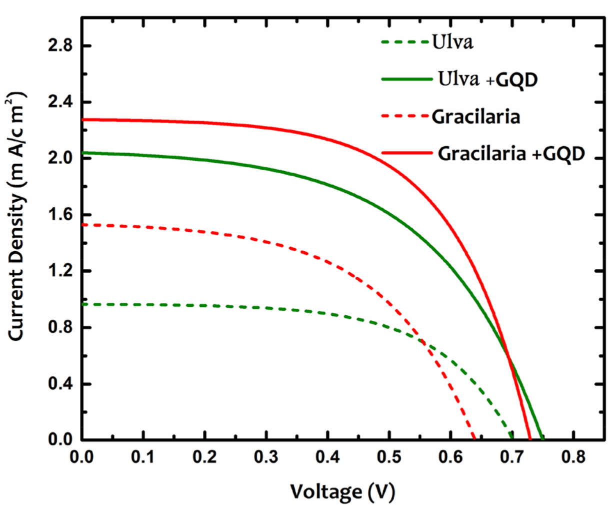

Fig. 10 *J–V* curve of natural dye-sensitized solar cells with dyes and dyes + GQD as photosensitizers

$$FF = (I_{mp} \times V_{mp})/(I_{sc} \times V_{oc}) = P_{max}/(I_{sc} \times V_{oc}). \quad (6)$$

Efficiency is associated with the ability of solar cells to produce the maximum amount of electricity from a light energy source. To calculate the efficiency of the cell, P_{out} is divided by P_{in} (the input power). The P_{out} should be P_{max} since the solar cell can be operated up to its maximum power output to get the maximum efficiency. It is obtained from the following equations (Gray 2020):

$$\text{Efficiency } (\eta) = P_{out}/P_{in} = P_{max}/P_{in}, \quad (7)$$

$$P_{max} = V_{max} \times I_{max}, \quad (8)$$

$$P_{in} = E \times A, \quad (9)$$

where E is the incident radiation flux in w/m^2 and A is the area of the cell.

From Fig. 10, the Gracilaria-based DSSC has a higher short circuit current density (J_{SC}) than the Ulva-based DSSC while having less open-circuit voltage (V_{OC}). The data for the natural dye-sensitized solar cells based on dyes and dyes + GQD are summarized in Table 2. As previously mentioned, higher efficiency of Gracilaria based compared to Ulva-based DSSC may be due to a broader absorption peak in the range of visible light that it can absorb more sunlight. For Gracilaria + GQD, the absorbed wavelength range is more than Ulva + GQD, which includes more wavelengths, resulting in more sunlight absorption and increasing efficiency. Furthermore, the DSSC, which has used natural dyes + GQD, both had more V_{OC} and higher J_{SC}. As expected, addition of GQDs to dye as a sensitizer raised the electron–hole separation rate and as a result, the J_{SC} is increased. This value for the Ulva + GQD compared to Ulva was approximately two times, i.e., significant as well as the efficiency of DSSC with Gracilaria + GQD and Ulva + GQD in comparison with Gracilaria and Ulva improved about 80% and 107%, respectively. The FF is one of the essential factors in DSSC, which is defined as the ratio of maximum obtained power to the produced open circuit voltage and short circuit current. The FF of all cells calculated in the range of 50–60% approximately, i.e., appropriate values. The best efficiency was obtained about 0.94% for the samples which Gracilaria + GQD was used as the sensitizer.

Table 2 Characteristics of natural dye-sensitized solar cells with dyes and dyes + GQD as photosensitizers

Dye	Molecular structure	V_{OC} (V)	J_{SC} *mA cm^{-2})	FF (%)	*H* (%)
Gracilaria	Phycobilin	0.64	1.52	53	0.52
Gracilaria + GQD	Phycobilin	0.73	2.26	56	0.94
Ulva	Chlorophyll	0.70	0.96	57	0.39
Ulva + GQD	Chlorophyll	0.75	2.04	52	0.81

The use of dyes extracted from seaweeds has reported, but mainly focused on chlorophyll-based dyes. To the best of our knowledge, there is no report for using Gracilaria or Ulva as the sensitizer in the literature. It has been reported that natural dye-based cells showed efficiencies values up to 2% with good stability (Calogero 2012, 2015; Calogero et al. 2014; Ananth et al. 2015; Shalini et al. 2015). Enciso et al. assembled dye-sensitized solar cells using red algae dye with the maximum efficiency of 0.045% (Enciso et al. 2016). Anand et al. utilized Sargassum wightii as a sensitizer in solar cell with 0.07% efficiency (Anand and Suresh 2015). Prabavathy et al. extracted anthocyanins and enhanced the solar cell efficiency from 0.99 to 1.47% (Prabavathy et al. 2018). Hiramoto et al. fabricated organic solar cell and its efficiency reached 0.7% (Hiramoto et al. 1991).

Conclusions

DSSCs were assembled using natural dyes extracted from the red (Gracilaria) and green (Ulva) algae as the sensitizers. The natural dyes with phycobilin and chlorophyll in plants can efficiently absorb light. The UV–Vis spectra of Gracilaria show it has an absorbent peak at about 530 nm, and chlorophyll-containing dye extracted from Ulva has a maximum absorption at 680 nm. PL analysis confirmed the reduction in electron–hole recombination. According to the data, the Gracilaria-based DSSC has higher J_{SC} than the Ulva-based DSSC while having less V_{OC}. Our result showed that adding GQDs to dye as a sensitizer increased the efficiency significantly and J_{SC}. The optimum energy conversion efficiency of approximately 0.94% has been achieved for DSSC with Gracilaria + GQD under the condition of irradiation of AM 1.5 (100 mW cm^{-2}) simulated sunlight, and J_{SC} was 2.26 mA.cm^{-2}, V_{OC} was 0.73 V, and FF was 56%.

This study suggests that the exploration of extensive marine seaweed resources to use as a sensitizer in a solar cell would be a low-cost, environment-friendly alternative to the expensive metal complexes. DSSC based on Gracilaria using GQD has higher efficiency compared with the reported organic solar cells.

Compliance with Ethical Standards

Conflict of interest There is no conflict of interest.

References

Aghelifar M, Kimiagar S (2018) pH effect on the size of graphene quantum dot synthesized by using pulse laser irradiation. Phys Chem Res 6(2):237

Ali B (2015) Decrease of back recombination rate in CdS quantum dots sensitized solar cells using reduced graphene oxide. Chin Phys B 24(4):047205

Anand M, Suresh S (2015) Marine seaweed Sargassum wightii extract as a low-cost sensitizer for ZnO photoanode based dye-sensitized solar cell. Adv Nat Sci Nanosci Nanotechnol 6(3):035008

Ananth S, Vivek P, Solaiyammal T, Murugakoothan P (2015) Pre dye treated titanium dioxide nano particles sensitized by natural dye extracts of Pterocarpus marsupium for dye sensitized solar cells. Optik 126:1027

Argazzi R et al (2004) Design of molecular dyes for application in photoelectrochemical and electrochromic devices based on nanocrystalline metal oxide semiconductors. J Photoch Photobio A 164(1–3):15

Bach U et al (1998) Solid-state dye-sensitized mesoporous TiO_2 solar cells with high photon-to-electron conversion efficiencies. Nature 395:583

Bessho T et al (2010) Highly efficient mesoscopic dye-sensitized solar cells based on donor–acceptor-substituted porphyrins. Angew Chem Int Edit 49(37):6646

Calogero G et al (2010) Efficient dye-sensitized solar cells using red turnip and purple wild sicilian prickly pear fruits. Int J Mol Sci 11(1):254

Calogero G et al (2012) Anthocyanins and betalains as light-harvesting pigments for dye-sensitized solar cells. Sol Energy 86(5):1563

Calogero G et al (2015) Vegetable-based dye-sensitized solar cells. Chem Soc Rev 44(10):3244

Calogero G, Citro I, Di Marco G, Minicante SA, Morabito M, Genovese G (2014) Self-assembly of organic nanomaterials and biomaterials: the bottom-up approach for functional nanostructures formation and advanced applications. Acta Part A Mol Biomol Spectrosc 117:702

Calogero G, Di Marco G (2008) Red Sicilian orange and purple eggplant fruits as natural sensitizers for dye-sensitized solar cells. Sol Energ Mat Sol C 92(11):1341

Dai Q, Rabani J (2002) Unusually efficient photosensitization of nanocrystalline TiO_2 films by pomegranate pigments in aqueous medium. New J Chem 26(4):421

Diao S, Zhang X, Shao Z, Ding K, Jie J, Zhang X (2017) Hue tunable, high color saturation and high-efficiency graphene/silicon heterojunction solar cells with MgF2/ZnS double anti-reflection layer. Nano Energy 31:359

Enciso P, Cerdá MF (2016) Solar cells based on the use of photosensitizers obtained from Antarctic red algae. Cold Reg Sci Technol 126:51

Fang X, Li M, Guo K, Li J, Pan M, Bai, et al (2014) Charge and energy transfer interplay in hybrid sensitized solar cells mediated by graphene quantum dots. Electrochim Acta 137:634

Gray JL (2020) The physics of the solar cell. Handbook of photovoltaic science and engineering, 2nd edn. Purdue University, West Lafayette, Indiana, USA

Gupta V, Chaudhary N, Srivastava R, Sharma GD, Bhardwaj R et al (2011) Luminscent graphene quantum dots for organic photovoltaic devices. J Am Chem Soc 133(26):9960

Hao S et al (2006) A thermoplastic gel electrolyte for stable quasi-solid-state dye-sensitized solar cells. Sol Energy 80(2):209

Hao Y et al (2016) Novel blue organic dye for dye-sensitized solar cells achieving high efficiency in cobalt-based electrolytes and by co-sensitization. ACS Appl Mater Inter 8(48):32797

Hiramoto M, Fujiwara H, Yokoyama M (1991) Morphological studies of organic photovoltaic blendsApplied physics letters. Appl Phys Lett 58(10):1062

Ho NT et al (2016) Enhancement of recombination process using silver and graphene quantum dot embedded intermediate layer for efficient organic tandem cells. Sci Rep 6:30327

Hu Y, Robertson N (2016) Molecular engineering of potent sensitizers for very efficient light harvesting in thin-film solid-state dye-sensitized solar cells. Front Optoelectron 9(1):38

Kongkanand A, Tvrdy K, Takechi K, Kano M, Kamat PV (2008) Quantum dot solar cells. Tuning photoresponse through size and shape control of CdSe−TiO_2 architecture. J Am Chem Soc 130(12):4007

Kroeze JE, Hirata N, Schmidt-Mende L, Orizu C, Ogier SD, Carr K et al (2006) Amphiphilic poly(vinyl chloride)-g-poly(oxyethylene methacrylate) graft polymer electrolytes: Interactions, nanostructures and applications to dye-sensitized solar cells. Adv Funct Mater 16(14):1832

Kuang D et al (2008) Evaluation of solution-processed reduced graphene oxide films as transparent conductors. ACS Nano 2(6):1113

Kundu S, Sarojinijeeva P, Karthick R, Anantharaj G, Saritha G, Bera R et al (2017) Synthesis of magnetically reusable Fe_3O_4 nanospheres-N, Sco-doped graphene quantum dots enclosed CdSe its application as a photocatalyst. Electrochim Acta 242:337

Long R (2013) Understanding the Electronic Structures of Graphene Quantum Dot Physisorption and Chemisorption onto the TiO_2 (110) Surface: A First-Principles Calculation. Chem Phys Chem 14(3):579

Lu J, Yeo PSE, Gan CK, Wu P, Loh KP (2011) Theoretical studies on the growth mechanism of chemical vapor deposition of graphene on metal surface. Nat Nanotechnol 6(4):247

Mahmood A (2016) Chitosan functionalized poly(vinyl alcohol) for prospects biomedical and industrial applications. Sol Energy 123:127

Mihalache I, Radoi A, Mihaila M, Munteanu C, Marin A, Danila M et al (2015) Intrinsic limitations of impedance measurements in determining electric double layer capacitances. Electrochim Acta 153:306

Najafi V, Aghelifar M, Kimiagar S (2017) A novel synthesis of CZTS quantum dots using pulsed laser irradiation. Superlattice Microst 109:702

Najafi V, Kimiagar S (2018) Cd-free Cu_2ZnSnS_4 thin film solar cell on a flexible substrate using nano-crystal ink. Thin Solid Films 657:70

Narayan MR (2012) Graphene oxide liquid crystals: discovery. Evolution and applications. ADV Mater Res-Switz 16(1):208

Nazeeruddin MK et al (2001) Engineering of efficient panchromatic sensitizers for nanocrystalline TiO_2-based solar cells. J Am Chem Soc 123(8):1613

Nguyen-Phan TD, Pham VH, Shin EW, Pham HD, Kim S, Chung, et al (2011) The role of graphene oxide content on the adsorption-enhanced photocatalysis of titanium dioxide/graphene oxide composites. Chem Eng J 170(1):226

O'Regan B, Grätzel M (1991) A low-cost, high-efficiency solar cell based on dye-sensitized colloidal TiO_2 films. Nature 353:737

Patterson A (1939) The Scherrer formula for X-ray particle size determination. Phys Rev 56(10):978

Paulo S, Palomares E, Martinez-Ferrero E (2016) Novel carbon quantum dots from egg yolk oil and their haemostatic effects. Nanomater Basel 6(9):157

Peng J, Gao W, Gupta BK, Liu Z, Romero-Aburto R, Ge L et al (2012) Graphene quantum dots derived from carbon fibers. Nano Lett 12(2):844

Prabavathy N, Shalini S, Balasundaraprabhu R, Dhayalan Velauthapillai S, Prasanna G, Muthukumarasamy BN (2018) Enhancement in the photostability of natural dyes for dye-sensitized solar cell (DSSC) applications. Int J Energy Res 42(2):790

Riesen H, Wiebeler C, Schumacher S (2014) Optical spectroscopy of graphene quantum dots: the case of C132. J Phys Chem A 118(28):5189

Ritter KA, Lyding JW (2009) Metal ion binding with carbon nanotubes and graphene: Effect of chirality and curvature. Nat Mater 8(3):235

Sathiyan G et al (2016) Review of carbazole based conjugated molecules for highly efficient organic solar cell application. Tetrahedron Lett 57(3):243

Schmidt-Mende L, Bach U, Humphry-Baker R, Horiuchi T, Miura H, Ito S et al (2005) Theoretical study of indoline dyes for dye-sensitized solarcells. Adv Mater 17(7):813

Shalini S, Balasundara P, Prasanna S, Tapas K, Senthilarasu S (2015) The colour rendering index and correlated colour temperature of dye-sensitized solar cell for adaptive glazing application. Renew Sust Energy Rev 51:1306

Smestad GP (1998) Education and solar conversion: demonstrating electron transfer. Sol Energ Mat Sol C 55(1):157

Snaith HJ, Grätzel M (2007) Recent trends in mesoscopic solar cells based on molecular and nanopigment light harvesters. Adv Mater 19(21):3643

Wallace J (2009) Temporal stability of blue phosphorescent organic light-emitting diodes affected by thermal annealing of emitting layers. University of Rochester

Wang Z-S et al (2004) Significant influence of TiO_2 photoelectrode morphology on the energy conversion efficiency of N719 dye-sensitized solar cell. Coordin Chem Rev 248(13–14):1381

Wolf M (1971) A new look at silicon solar cell performance. Energy Convers 11:63

Wu J, Lan Z, Lin J, Huang M, Huang Y, Fan L et al (2015) Electrolytes in dye-sensitized solar cells. Chem Rev 115(5):2136

Zhao Q, Xie T, Peng L, Lin Y, Wang P, Peng L et al (2007) Size-and orientation-dependent photovoltaic properties of ZnO nanorods. J Phys Chem C 111(45):17136

Zhu Z, Ma J, Wang Z, Mu C, Fan Z, Du L et al (2014) Efficiency enhancement of Perovskite solar cells through fast electron extraction: the role of graphene quantum dots. J Am Chem Soc 136(10):3760

Zhu C, Yang S, Wang G, Mo R, He P, Sun J et al (2015) A new mild, clean and highly efficient method for the preparation of graphene quantum dots without by-products. J Mater Chem B 3(34):6871

Zhu S, Zhang J, Qiao C, Tang S, Li Y, Yuan W et al (2011) Strongly green-photoluminescent graphene quantum dots for bioimaging applications. Chem Commun 47:6858

Zhu S, Zhang J, Tang A, Qiao C, Wang L, Wang H et al (2012) Photoluminescence mechanism in graphene quantum dots: Quantum confinement effect and surface/edge state. Adv Funct Mater 22:4732